Journal of Molecular Structure 918 (2009) 101–107

Contents lists available at ScienceDirect

Journal of Molecular Structure

journal homepage: www.elsevier.com/locate/molstruc

1,3-Dibenzylimidazolium salts: A paradigm of water and anion effect on the supramolecular H-bonds network

Loïc Leclercq, Michel Simard, Andreea R. Schmitzer *

Université de Montréal, Département de Chimie, CP 6128 Succursale Centre Ville, Montréal, Que., Canada H3C 3J7

ARTICLE INFO

Article history:
Received 10 July 2008
Accepted 21 July 2008
Available online 31 July 2008

Keywords:
1,3-Dibenzyl imidazolium salts
Crystal structure
Imidazolium
X-rays
Supramolecular organization
Hydrogen bonds

ABSTRACT

Two crystals of 1,3-dibenzylimidazolium salts with chloride (crystal **I**) and hexafluorophosphate (crystal **III**) have been obtained by slow evaporation of a saturated aqueous solution for **I** and saturated chloroform solution for **III**. The two structures are described and compared to the corresponding bromide salt (crystal **II**). The X-ray diffraction studies on single crystals revealed that the three crystalline materials are monoclinic with $P2_1/n$ or $P2_1/c$ space group. The structures of **I** and **III** are completely different compared to that of the analogous bromide salt (**II**): no C—H···π or π–π interactions were observed and only very weak H-bonds occur between the acidic protons of the imidazolium ring and the halogenated atoms of the anion for compound **III**. For **I** and **II**, water molecules are included in the crystal lattice. Water molecules link the chloride anions in the case of **I**, but there are no direct interactions between the protons of the imidazolium ring and water molecules, as in the case of compound **II**. The hydrogen bond network in the case of compound **II** is formed *via* water molecules between the cations and the anions. In the case of the hexafluorophosphate salt, classical organization in an extended network of cations and anions connected together by hydrogen bond was observed.

1. Introduction

Ionic liquids (ILs) are an attractive field in chemistry. These salts are defined as "molten salts" with melting points below 100 °C. The significant interest in ILs is due to their chemical characteristics and potentially useful solvent properties [1,2]. The most common ILs are members of the 1,3-disubstituted imidazolium family, which generally have been used as green solvents in organic synthesis, organometallic catalysis and enzymatic catalysis [3–11]. Many applications also exist in separation processes, nano-chemistry, electrochemistry and as new materials [12–14]. Recent studies have demonstrated that pure 1,3-disubstituted imidazolium salts form a hydrogen-bonded supramolecular network in the solid phase. The H-bonds are proposed to be maintained, to a great extent, in the liquid or gas phase [15]. The imidazolium salts possess pre-organized structures: through the three acidic protons localized on the imidazolium ring that can act as H-bond donors, and *via* π-stacking in the third dimension (Fig. 1) [15]. In fact, an overview of the X-ray studies reported in the past decade on the structure of 1,3-dialkylimidazolium salts [16–20], reveals that they form an extended network of cations and anions connected together by hydrogen bonds. The monomeric unit is always composed of one imidazolium cation surrounded by at least three anions and each anion is surrounded by at least three imidazolium cations [21]. The strongest hydrogen bond always involves the most acidic H_2 ($pK_a = 23.0$ for the 1,3-dimethylimidazolium cation) [22,23] followed by H_4 and H_5 of the imidazolium ring. These hydrogen bonds are weak to moderate (with H···X bond lengths > 2.2 Å; C—H···X bond angles between 100° and 180°) [24]. The number of anions that surround the cation (and vice-versa) varies according to the anion size and the nature of the imidazolium residues.

We have recently reported the self-assembly of 1,3-dibenzylimidazolium halides in solution and in gas phase, on the basis of NMR titrations, mass spectrometry data and theoretical calculations [25]. The benzyl groups impose additional π-stacking interactions with the imidazolium rings by aromatic stacking (T or π). In solution, the chloride salt has a similar organization to its bromide analogue. The crystal structure of 1,3-dibenzylimidazolium bromide revealed an atypical organization when compared to previously observed structures of ILs [25]. Since water molecules participate directly in the formation of the supramolecular network, a fact very unusual for imidazolium salts, we were inspired to perform a crystallographic study of the 1,3-dibenzylimidazolium analogs, namely the chloride and the hexafluorophosphate. To simplify the notation, the crystals of the 1,3-dbenzylimidazolium salts are referred to as **I**, **II** and **III**, for chloride, bromide and hexafluorophosphate anions, respectively (Fig. 2).

---

* Corresponding author. Tel.: +1 514 343 6744; fax: +1 514 343 7586.
E-mail address: ar.schmitzer@umontreal.ca (A.R. Schmitzer).

0022-2860/$ - see front matter © 2008 Elsevier B.V. All rights reserved.
doi:10.1016/j.molstruc.2008.07.023

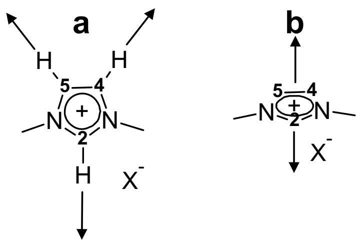

Fig. 1. (a) The three T-stacking and H-bond donors of an imidazolium ring and their directionality, and (b) π-stacking.

2. Experimental

2.1. Materials

All reactions were carried out in oven-dried glassware under nitrogen, using standard Schlenk and vacuum line techniques. The ^{1}H and ^{13}C NMR spectra were recorded using an Advance 300 Brucker, at 300.13 and 75.49 MHz, respectively. Chemical shifts are given in ppm (δ) and measured relative to residual solvent. Elemental analyses were performed by the "Université de Montréal" facility. $CDCl_3$ and all other chemicals were purchased from Aldrich and used without further purification. "Distilled" solvents were obtained using a GlassContour system (Irvine, CA).

2.2. Synthesis of 1,3-dibenzylimidazolium chloride (**I**)

A dry flask (250 mL), equipped with a magnetic stir bar and a septum-inlet for nitrogen, was charged with a solution of (chloromethyl) benzene (1.06 g, 8.42 mmol) in toluene (50 mL). In a Schlenk, a solution of 1-benzylimidazole (1.60 g, 10.1 mmol) in toluene (10 mL) was added to the other flask in a dropwise fashion by cannulation at 0 °C. The reaction mixture was stirred for 20 min at room temperature, then filtered under gravity. The solid was washed with diethylether to remove unreacted 1-benzylimidazole. The white solid was dried overnight at 120 °C in a vacuum. The product was stored under dry nitrogen (90%).

^{1}H NMR (300 MHz, $CDCl_3$, 20 °C, TMS): δ = 5.41 (s, 4H, NCH_2), 7.23 (m, 6H, $H_{aro(ortho)}$, $H_{aro(para)}$ and imidazolium CH=CH), 7.34 (d, 2H, CH=CH, $^3J_{H-H}$ = 1.3 Hz), 7.41 (dd, 4H, $H_{aro(meta)}$, $^3J_{H-H}$ = 6.3 Hz and $^3J_{H-H}$ = 6.7 Hz), 10.92 ppm (s, 1H, N=CHN); ^{13}C NMR (75 MHz, $CDCl_3$, 20 °C): δ = 53.0 ppm (NCH_2), 122.0 ppm (CH=CH), 128.7 ppm (C_m), 129.1 ppm (C_o), 129.2 ppm (C_p), 133.0 ppm (N=CHN), 137.0 ppm ($C_{aro}CH_2$). Anal. Calc. for $C_{17}H_{17}ClN_2$: C, 71.70%; H, 6.02%; N, 9.84%. Found: C, 69.89%; H, 6.01%; N, 9.75%. ESI/HRMS *m/z* found: 249.1582 $(M-Cl)^+$, calc.: 249.1391. MP: 63 °C.

2.3. Synthesis of 1,3-dibenzylimidazolium bromide (**II**)

The procedure is identical to the one which presented above.

^{1}H NMR (300 MHz, $CDCl_3$, 25 °C, TMS): δ (ppm) = 5.52 (s, 4H, NCH_2), 7.23 (d, 2H, CH=CH, $^3J_{H-H}$ = 1.4 Hz), 7.31–7.39 (m, 10H; H_{aro}), 10.51 (s, 1H; N=CHN); ^{13}C NMR (75 MHz, $CDCl_3$, 25 °C): δ (ppm) = 53.2 (NCH_2), 121.8 (CH=CH), 128.9 (C_m),129.3 (C_o), 129.3 (C_p), 132.7 (NCHN), 136.6 ($C_{aro}CH_2$). Anal. Calc. for $C_{17}H_{17}BrN_2$; $2H_2O$: C, 55.90%; H, 5.79%; N, 7.67%. Found: C, 54.84%; H, 5.77%; N, 7.87%. ESI/HRMS *m/z* found: 249.1376 $(M-Br)^+$, calc.: 249.1391. MP: 85 °C.

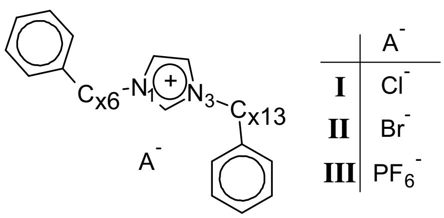

Fig. 2. The three crystals studied in this work (for **I** and **II** (x = 0), for **III** cation 1 (x = 1) and for **III** cation 2 (x = 2)).

2.4. Synthesis of 1,3-dibenzylimidazolium hexafluorophosphate (***III***)

The 1,3-dibenzylimidazolium bromide salt was dissolved in water (5 mmol L^{-1}) and a NH_4PF_6 aqueous solution (5 mmol L^{-1}) was added. The imidazolium hexafluorophosphate salt precipitates (95%).

^{1}H NMR (300 MHz, $CDCl_3$, 25 °C, TMS): δ (ppm) = 5.23 (s, 4H, NCH_2), 7.24 (m, 2H, CH=CH, $^3J_{H-H}$ = 1.3 Hz), 7.3–7.4 (m, 10H; H_{aro}), 9.63 (s, 1H; N=CHN); ^{13}C NMR (75 MHz, $CDCl_3$, 25 °C): δ (ppm) = 53.2 (NCH_2), 121.4 (CH=CH), 128.6 (C_m),129.1 (C_o), 129.3 ppm (C_p), 132.5 (N=CHN), 136.2 ($C_{aro}CH_2$). Anal. Calc. for $C_{17}H_{17}F_6N_2P$: C, 51.78%; H, 4.35%; N, 7.10%. Found: C, 51.82%; H, 5.41%; N, 7.11%. ESI/HRMS *m/z* found: 249.1264 $(M-PF_6)^+$, calc.: 249.1391. MP: 93 °C.

2.5. Crystallization and X-ray diffraction

All the crystallizations are performed in an open flask by dissolving the 1,3-dibenzylimidazolium cation (33 wt.%) in 10 mL of hot water (for **I** and **II**) or in 10 mL of hot chloroform (for **III**). After a week at room temperature, single crystals suitable for X-ray diffraction were obtained. All X-ray data were collected at T = 150 K and the structures were solved by the direct method with ShelxS-97. All non-H atoms were refined by full-matrix least-squares with anisotropic displacement parameters while hydrogen atoms were placed in idealized position. Hydrogen atoms from the water molecules were initially located from a difference Fourier map, then their location were adjusted using restrains at idealized distances (0.84 Å) and angles (104.5°) in the direction of the hydrogen bonding acceptors, either chloride (compound **I**) or bromide (compound **II**) anions.

X-ray crystallographic data for **I** and **III** were collected from a single crystal sample, which was mounted on a loop fiber. Data were collected using a Bruker microstar diffractometer equipped with a Platinum 135 CCD Detector, Helios optics and Kappa goniometer. The crystal-to-detector distance was 4.0 cm, and the data collection was carried out in 512 × 512 pixel mode. The initial unit cell parameters were determined by a least-squares fit of the angular setting of strong reflections, collected by a 10.0° scan in 33 frames over three different parts of the reciprocal space (99 frames total). One complete sphere of data was collected.

X-ray crystallographic data for **II** were collected from a single crystal sample, which was mounted on a loop fiber. Data were collected using a Bruker Platform diffractometer, equipped with a Bruker SMART 4K Charged-Coupled Device (CCD) Area Detector using the program APEX II and a Nonius FR591 rotating anode equipped with Montel 200 optics. The crystal-to-detector distance was 5.0 cm, and the data collection was carried out in 512 × 512 pixel mode. The initial unit cell parameters were determined by the same procedure (see above). One complete sphere of data was collected, to better than 0.80 Å resolution.

In each case, the refinement was on F^2 using all reflections. The weighted R-factor (wR) and goodness-of-fit S are based on F^2, conventional R-factors (R) are based on F, with F set to zero for negative F^2. The threshold expression of $F^2 > 2\sigma(F^2)$ is used only for calculating R-factors (gt) etc. and is not relevant to the choice of reflections for refinement. All esds (except the eds in the dihedral angle between two l.s. planes) are estimated using the full covariance matrix.

3. Results and discussion

3.1. Crystal packing of 1,3-dibenzylimidazolium chloride (**I**)

The synthesis of **I** is achieved through substitution on benzyl chloride by 1-benzylimidazole in a dry flask under positive nitrogen pressure in anhydrous toluene [2]. The reaction proceeds in 90% yield. The chloride salts are air stable but very hygroscopic and stored in sealed Schlenks.

Crystallization of **I** was carried out efficiently from hot water. An aqueous solution of **I** (33 wt.%) was heated until homogenization and then left at room temperature. Relatively small needle crystals ($0.15 \times 0.10 \times 0.05$ mm) suitable for X-ray analysis were obtained. The single crystals crystallized in a monoclinic system with a $P2_1/n$ space group (see Fig. 3 and Table 1).

The cations of **I**, **II** and **III** can be described as an imidazolium rigid unit linked by flexible methylene bridges to two aromatic rings. The two benzyl groups around the planar imidazolium unit adopt an *anti* conformation. Table 2 indicates the angles between the two benzyl groups for compounds **I**, **II** and **III**.

The orientation of the two $N—CH_2—C$ bridges to the planar imidazolium unit are different from one side to the other. Interplane angles of 81.9(2)° on the C_6 side and 41.7(1)° on the C_{13} side were found for **I.** The orientation of one of the phenyl groups is closer to the plane of the central imidazolium unit. The two phenyl rings are oriented almost perpendicular to the imidazolium planar unit, as shown by the 76.0(2)° and 80.0(1)° interplane angles.

The supramolecular organization of cations and anions in the crystal lattice of **I** is similar to the previously reported 1,3-dialkyl imidazolium salts, *i.e.* the acidic protons of the imidazolium ring form H-bonds with the chloride anions (Table 3) [15,21].

Interestingly, the strongest H-bonds are observed for the H_5 and the Cl_1 anion (angle $C_5—H_5\cdots Cl_1$ of 157° and $H_5\cdots Cl_1$ distance of 2.49 Å) and not between the most acidic H_2 and the Cl_1 anion (angle $C_2—H_2\cdots Cl_1$ of 122° and $H_2\cdots Cl_1$ distance of 2.82 Å). Two chlorides were found to be linked by H-bonds *via* two water molecules forming a diamond pattern (Fig. 4a). This elemental structure can be seen as a clathrate formed by H-bonds. The other weak hydrogen bonds between H_2 and Cl_1 link the clathrathes in the solid state. The 3D structure of **I** can be described as chains of imidazolium cations but the distance between them is around 8.4 Å. However a partial overlapping occurs between the phenyl groups and the imidazolium cation, positioned at a 3.7 Å distance. The main forces in this 3D organization are the hydrogen bonds between the water molecules and chloride ions that connect in the same time the H(2) imidazolium proton (Fig. 4b).

3.2. Crystal packing of 1,3-dibenzylimidazolium bromide (**II**)

The synthesis and the crystallization of **II** have been previous reported (Fig. 5 and Table 1 for structure information). We report here only the geometric aspect of the crystal packing of **II.** The crystalline system for the chloride and the bromide salts are identical (monoclinic) with a space group of $P2_1/c$ for bromide and $P2_1/n$ for chloride. It is worth noting that for both **I** and **II**, water molecules are present in the lattice suggesting that cohesion of the crystal is not ensured only by the presence of the two ions.

At the molecular level, the cation of compound **II** is also adopting an *anti* conformation of the benzyl groups around the imidazolium rigid unit. The orientation of the two $N—CH_2—C_{ar}$ bridges to the imidazolium plane are similar; as demonstrated by the angles of 84.6(1)° for the C_6 side and 80.0(1)° for the C_{13} side. These two large interplane values are an indication that the phenyl groups are oriented away from the plane of the central imidazolium unit. The orientation of the two aromatic rings related to the central imidazolium unit are found to be largely different for the two sides, as angles of 79.1(1)° and 45.0(2)° were observed.

The crystal structure of **II** reveals an atypical supramolecular network organization of cations and anions, compared to the chloride salt and other imidazolium salt crystals [15,21]. In fact, in the present system (**II**), the hydrogen bond network is formed *via* water molecules between the cations and the anions. Each imidazolium is surrounded closely by two water molecules and each water molecule interacting directly with two anions. Very weak to moderate hydrogen bonds [26] ($H\cdots X > 2.2$ Å and $Y—H\cdots X$ between 140° and 170°) can be observed in the crystal (Table 4 and for more information, see Ref. [25]).

It is important to notice that a very weak hydrogen bond between H_2 and an oxygen atom of a water molecule is present ($C—H\cdots O > 2.79$ Å; $C—H\cdots O$ of 146°). In this structure, such hydrogen bonds are unusual and indicate that: (i) the protons of the imidazolium ring are not interacting directly with the anions but *via* interactions with water molecules ($H_{2'}\cdots O_{1'}$ and $H_{4'}\cdots O_{1''}$), and (ii) the H_4 proton is involved in a weak hydrogen bond with a water molecule ($H_{4'}\cdots O_{1''}$). Moreover, the 2D structure can be partially described as chains formed *via* hydrogen bonds of water molecules and bromide ions (Fig. 6). The distance between two adjacent phenyl rings (of two different cations) is approximately 3.7 Å but the orbital overlap is non-existent. However, the distance between an imidazolium (π-deficient) and a phenyl ring (π-rich) is approximately 3.4 Å, indicative of a strong π-stacking interaction between the two rings. Another important stacking interaction was observed in the crystalline structure: T-stacking occurs between the H_5 proton (a partially positively charged hydrogen atom) and the phenyl ring. In fact, the H_5 proton points perpendicularly to the center of the phenyl plane (the distance is approximately 2.7 Å) (Fig. 6 and for more information see Ref. [25]).

Indeed, the 3D arrangement of the molecules in the crystal structure is formed by two 2D networks, the first one being composed of bromide anions and water molecules and the second one occurring by T-stacking between the imidazolium and the phenyl rings. The principal interaction (the T-stacking) governs the formation of a dimer, included in the bromide/water network (Fig. 6). Overall, both hydrogen bonds and aromatic stacking interactions play key role in the assembly of this structure.

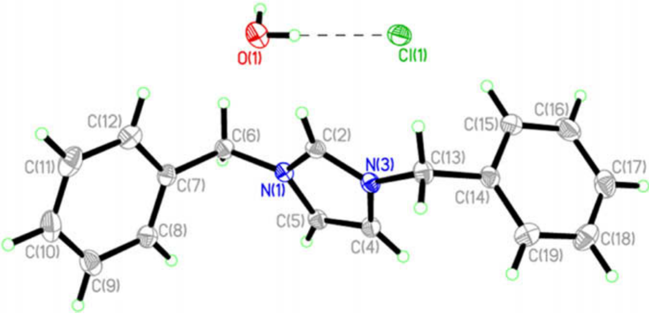

Fig. 3. ORTEP view of **I** with the numbering scheme adopted. Ellipsoids drawn at 30% probability level.

3.3. Crystal packing of 1,3-dibenzylimidazolium hexafluorophosphate (***III***)

The synthesis of the imidazolium salt (**III**) has been previously described [2]. The anion metathesis of **II** is realized through stirring an aqueous solution of **II** with NH_4PF_6 salt to provide **III** in 90% yield.

Crystallization of the imidazolium hexafluorophosphate salt was carried out efficiently from hot chloroform. A chloroform solution of the imidazolium salt (33 wt.%) was heated until homogeni-

Table 1
Crystal data of crystals **I**, **II** and **III**

Compounds	**I**[a]	**II**[b]	**III**[a]
Cation formula	$C_{17}H_{17}N_2$	$C_{17}H_{17}N_2$	$C_{17}H_{17}N_2$
Anion formula	Cl	Br	PF_6
Water	H_20	H_20	–
Molecular weight	302.79	347.25	394.30
Crystal system	Monoclinic	Monoclinic	Monoclinic
Space groups	$P2_1/n$	$P2_1/c$	$P2_1/c$
a (Å)	13.4538 (3)	12.9952 (4)	9.9320 (2)
b (Å)	8.3964 (2)	11.6158 (3)	18.9782 (3)
c (Å)	14.8952 (3)	10.5961 (3)	18.7355 (3)
α (°)	90	90	90
β (°)	108.333 (2)	91.677 (2)	94.751 (2)
δ (°)	90	90	90
V (Å^3)	1597.21 (6)	1598.79 (8)	3519.35 (11)
Z	4	4	8
Color	Colorless	Colorless	Colorless
Crystal dim. (mm)	0.15 × 0.10 × 0.05	0.20 × 0.18 × 0.16	0.29 × 0.08 × 0.04
μ (mm^{-1})	2.111	3.500	1.990
Temperature (K)	150 (2)	150 (2)	150 (2)
$D_{calc.}$ (Mg m^{-3})	1.259	1.443	1.488
$F(000)$	640	712	1616
Theta range for collection (°)	6.13 and 67.82	3.04 and 73.05	3.32 and 67.94
Limiting indices	$-15 \leqslant h \leqslant 15$	$-14 \leqslant h \leqslant 15$	$-10 \leqslant h \leqslant 9$
	$-10 \leqslant k \leqslant 10$	$-14 \leqslant k \leqslant 14$	$-22 \leqslant k \leqslant 22$
	$-17 \leqslant l \leqslant 17$	$-12 \leqslant l \leqslant 13$	$-22 \leqslant l \leqslant 22$
Reflections collected/unique	25617/2572	21728/3146	55610/5918
R_{int}	0.035	0.036	0.043
Completeness to theta max. (%)	89.0	91.1	92.5
Data/restraints/parameters	2572/3/196	3146/3/197	5918/0/469
Final R indices [$I > 2\sigma(I)$]			
R_1	0.0326	0.0453	0.0442
wR_2	0.0907	0.1062	0.1141
R indices (all data)			
R_1	0.0332	0.0455	0.0474
wR_2	0.0913	0.1063	0.1169
Goodness-of-fit on F^2	1.033	1.246	1.062
Largest diff. peak and hole/e A^{-3}	0.245; −0.171	0.489; −1.266	0.515; −0.523

[a] Diffractometer: Bruker microstar equipped with a Platinum 135 CCD Detector, a Helios optics and a Kappa goniometer, absorption correction: empirical (SADABS), refinement method: full-matrix least-squares on F^2.

[b] Diffractometer: Bruker Platform, equipped with a Bruker SMART 4 K Charged-Coupled Device (CCD) area detector using the program APEX II and a Nonius FR591 rotating anode equipped with Montel 200 optics.

Table 2
Inter planes normal angles (angles (°))

	I		**II**		**III** (cation 1)		**III** (cation 2)	
n	6	13	6	13	16	113	26	213
Angle between N—C_{xn}—C and imidazolium ring[a]	81.9(2)	41.7(1)	84.6(1)	80.0(1)	53.0(2)	73.0(2)	54.4(2)	78.7(2)
Angle between N—C_{xn}—C and phenyl ring[a]	76.0(2)	80.0(1)	79.1(1)	45.0(2)	27.9(2)	59.2(2)	71.2(2)	34.4(2)
Angle between N—C_{x6}—C and N—C_{x13}—C[a]	51.0(2)		40.3(2)		40.7(3)		59.2(2)	

[a] For **I** and **II** ($x = 0$), for **III** cation 1 ($x = 1$) and for **III** cation 2 ($x = 2$).

Table 3
Distances and angles of Y—H···X hydrogen bonds in **I**[a]

	Y···H (Å)	H···X (Å)	Y···X (Å)	Y—H···X (°)	Symmetry operators for X
C_2—H_2···Cl_1	0.95	2.82	3.410 (2)	122	x, y, z
C_5—H_5···Cl_1	0.95	2.49	3.550 (2)	157	$1/2 + x, 1/2 - y$, ½+z
O_1—H_{1A}···Cl_1	0.840 (9)	2.363 (9)	3.2026 (2)	176 (2)	x, y, z
O_1—H_{1B}···Cl_1	0.839 (9)	2.413 (10)	3.2405 (12)	169 (2)	$1 - x, -y, 1 - z$

[a] Only H···X that have significant interactions are reported.

zation and then left at room temperature. Relatively small needles crystals (0.29 × 0.08 × 0.04 mm) suitable for X-ray analysis were obtained. The single crystals crystallized in a monoclinic system with a $P2_1/c$ space group (see Fig. 7 and Table 1).

The asymmetric unit of the crystal structure of compound **III** is composed of two imidazolium cations and two hexafluorophosphate anions. We adopted here the atom numbering of **III** by using the first digit of the atom's labeling as indication of the corresponding moiety. The two hexafluorophosphate anions were found to possess typical distances (range of 1.558–1.602 Å) and angles (range of 88.2–92.1°) around the central phosphor atom. The *anti* conformation of the two benzyl groups is still observed for the two cations of **III**. The orientations of the two N—CH_2—C_{ar} bridges from the central imidazolium unit are similar for both cations, as angles of 53.0(2)° and 73.0(2)° and, respectively, 54.4(2)° and 78.7(2)° are observed.

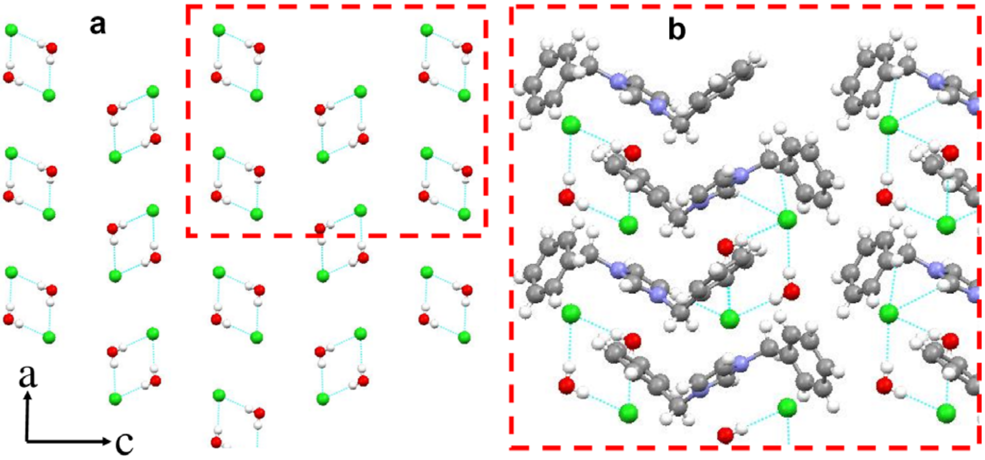

Fig. 4. (a) Network and (b) dimer for crystal **I** (H-bonds in blue for the dimeric structure). (For interpretation of the references to colour in this figure legend, the reader is referred to the web version of this paper.)

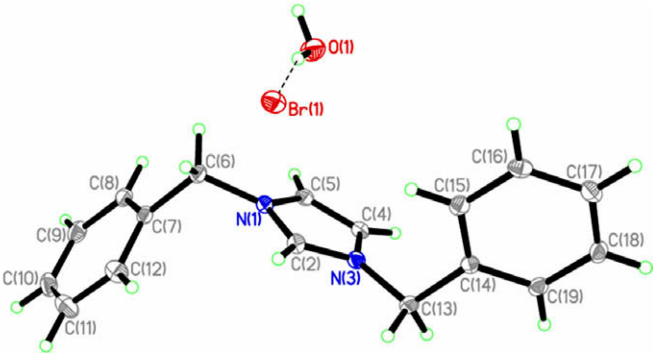

Fig. 5. ORTEP view of **II** with the numbering scheme adopted. Ellipsoids drawn at 30% probability level.

The crystal structure of **III** reveals a classical supramolecular organization as was reported for the other imidazolium salts, *i.e.* an extended 3D network of cations and anions connected together by hydrogen bonds [21]. From this point of view, compound **III** is completely different from the chloride and bromide analogs, as no water or chloroform molecules are present in the crystal lattice. The hydrogen bond network between the cations and the anions is very weak according to published criteria [16,26,27]. Each imidazolium is surrounded closely by six anions, but only two of them interact with very weak hydrogen bonds (2.3 Å < H···F < 2.6 Å; C—H···F between 140° and 172°; see Table 5).

From a supramolecular point of view, the structure can be described as a supramolecular filament of two imidazolium cations connected *via* a hexafluorophosphate anion. All filaments are intimately linked to form the crystalline network (Fig. 8). No stacking

Table 4
Distances and angles of Y—H···X hydrogen bonds in **II**[a]

	Y···H (Å)	H···X (Å)	Y···X (Å)	Y—H···X (°)	Symmetry operators for X
$C_2—H_2···O_{1'}$	0.95	2.79	3.616 (2)	146	*x*, 3/2−*y*, 1/2+*z*
$C_4—H_4···O_{1''}$	0.95	2.30	3.171 (2)	152	2−*x*, 1−*y*, −*z*
$O_1—H_{1A}···Br_1$	0.8399 (1)	2.528 (5)	3.3544 (16)	169 (2)	*x*, *y*, *z*
$O_1—H_{1B}···Br_1$	0.840 (1)	2.590 (7)	3.4092 (18)	165 (2)	*x*, 3/2 − *y*, −1/2 + *z*

[a] Only H···X that have significant interactions are reported.

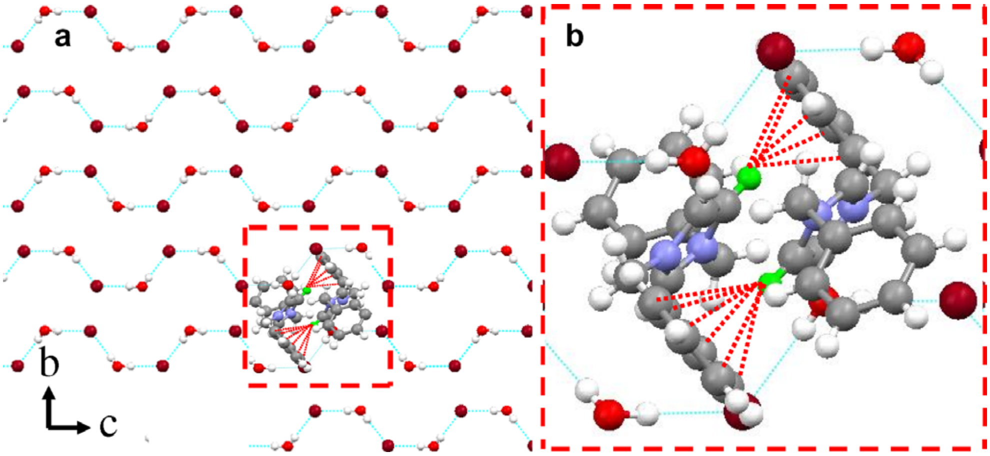

Fig. 6. (a) Network and (b) dimer for crystal **II** (H_5 appears in green, H-bonds in blue and T-stacking in red). (For interpretation of the references to colour in this figure legend, the reader is referred to the web version of this paper.)

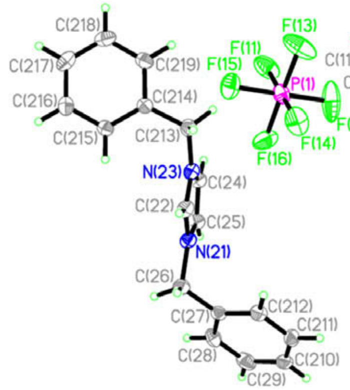

Fig. 7. ORTEP view of **III** with the numbering scheme adopted. Ellipsoids drawn at 30% probability level.

Table 5
Distances and angles of C—H⋯F hydrogen bonds in **III**[a]

	C⋯H (Å)	H⋯F (Å)	C⋯F (Å)	C—H⋯F (°)	Symmetry operators for F
C_{12}—H_{12}⋯F_{25}	0.95	2.51	3.329 (3)	144	1 − *x*, −*y*, 1 − *z*
C_{12}—H_{12}⋯F_{26}	0.95	2.30	3.119 (3)	144	1 − *x*, −*y*, 1 − *z*
C_{15}—H_{15}⋯F_{21}	0.95	2.58	3.500 (3)	164	2 − *x*, −*y*, 1 − *z*
C_{15}—H_{15}⋯F_{22}	0.95	2.47	3.252 (3)	140	2 − *x*, −*y*, 1 − *z*
C_{22}—H_{22}⋯F_{23}	0.95	2.38	3.210 (3)	146	1 − *x*, 1/2 + *y*, 3/2 − *z*
C_{24}—H_{24}⋯F_{13}	0.95	2.50	3.440 (3)	172	1 − *x*, 1 − *y*, 1 − *z*

[a] Only H⋯F that have significant interactions are reported.

interactions can be observed in this structure, which is in contrast to the crystal structure of the bromide salt **II**. This could be due to the larger steric bulk of the hexafluorophosphate compared to bromide anion.

*3.4. Comparison of crystals **I**, **II** and **III***

The large range in values of the torsion angles from the imidazolium central unit C_2—N—CH_2—C (phenyl) can be attributed mainly to the mixed sp^3 hybridization of the —CH_2— bridges and the sp^2 hybridization of the vicinal atoms (N-imidazolium, C-phenyl). This mixed hybridization adds flexibility to the cation, allowing a higher range of possible conformational angles. Table 6 reports the torsion angles obtained in the imidazolium cations of **I**, **II** and **III**. It is important to notice that the anion's size cannot be correlated with the imidazolium cation's conformation.

Table 6
Torsion angles related to the conformation of the cations (angles in °.)

	I	**II**	**III** (cation 1)	**III** (cation 2)
Imidazolium core to —CH_2— bridge conformation				
C_{x2}—N_{x1}—C_{x6}—C_{x7}[a]	−82.2(2)	−96.2(2)	−55.1(3)	−127.2(2)
C_{x2}—N_{x3}—C_{x13}—C_{x14}[a]	−138.6(2)	−100.4(1)	−106.5(2)	−99.2(3)
—CH_2— Bridge to phenyl ring conformation				
N_{x1}—C_{x6}—C_{x7}—C_{x8}[a]	−77.0(2)	−101.8(2)	−29.0(3)	−109.6(2)
N_{x1}—C_{x6}—C_{x7}—C_{x12}[a]	104.8(2)	79.5(2)	153.0(2)	71.6(3)
N_{x3}—C_{x13}—C_{x14}—C_{x15}[a]	80.0(2)	46.5(2)	59.4(3)	36.4(3)
N_{x3}—C_{x13}—C_{x14}—C_{x19}[a]	−99.3(2)	−136.3(2)	−120.7(2)	−147.2(2)

[a] For **I** and **II** (*x* = 0), for **III** cation 1 (*x* = 1) and for **III** cation 2 (*x* = 2).

It is interesting to compare the cation packing of the 1,3-dibenzylimidazolium moiety in the hexafluorophosphate salt (**III**) with that of its chloride or bromide analog (**I** and **II,** respectively). All have melting points below 100 °C but **I** or **II** crystallizes with two water molecules in the lattice. X-ray crystallographic studies show that both structures are dominated by electrostatic cation–anion interactions as are all the classical imidazolium salts [21]. However, for **II**, supplementary stacking interactions (π and T) can be observed, resulting in a dimeric structure in the solid state. Moreover, no direct H-bonds between cations and anions are observed in this case, but water molecules connect anions and cations. For **I**, only H-bonds are observed, with the strongest H-bond occurring between H_5 and a chloride anion and not between the most acidic proton (H_2) and the anion. The presence of water molecules assure the H-bond interaction between the imidazolium chains formed by π-stacking. For **III**, the most important difference compared to **I** and **II** is the absence of both stacking and H-bonds (those that can be observed are very weak). We propose that the size of the hexafluorophosphate anion may disrupt the cation–cation stacking and does not allow the imidazolium cations to dimerize.

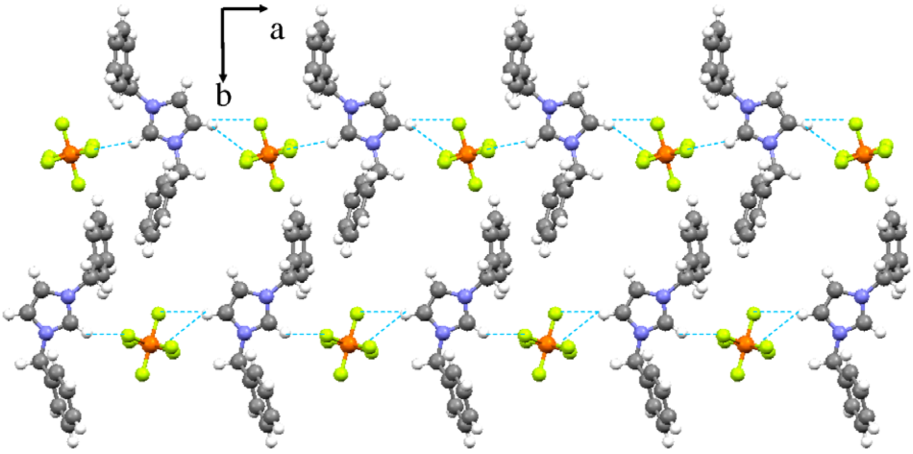

Fig. 8. View of H-bonds in crystal **III** (H-bonds in blue). (For interpretation of the references to colour in this figure legend, the reader is referred to the web version of this paper.)

4. Conclusion

In summary, the detailed structures of two new 1,3-dibenzylimidazolium salts with a chloride and a hexafluorophosphate anion (**I** and **III**, respectively), have been obtained. Given the precise X-ray crystal data, we are now able to understand the structural organization obtained previously with the bromide anion (compound **II**). The structure of the anion (as well as the structure of the cation, not studied here) is essential in dictating the self assembly of the cations, the anions (and eventually the inclusion of water molecules) in the solid state. Due to the current interest in the development of new supramolecular crystalline structures (molecular tectonics), this knowledge can aid in the design of self-assembly of imidazolium cations and anions to form highly organized structures.

Acknowledgements

The authors thank the Natural Sciences and Engineering Research Council of Canada, the Fonds Quebécois de la Recherche sur la Nature et les Technologies, the Canada Foundation for Innovation and Université de Montréal for financial support.

Appendix A. Supplementary data

Supplementary data associated with this article can be found in the online version. CCDC-688096 (**I**), 665763 (**II**), and 688095(**III**) contain the Supplementary crystallographic data for this paper. These data can be obtained free of charge from the Cambridge Crystallographic Data Centre *via* www.ccdc.cam.ac.uk/data_request/cif. Supplementary data associated with this article can be found, in the online version, at doi:10.1016/j.molstruc.2008.07.023.

References

[1] R.D. Rogers, K.R. Seddon, in: Ionic Liquids as Green Solvents; Progress and Prospects, ACS Symposium Series, vol. 856, American Chemical Society, Washington, DC, 2003.

[2] P. Wasserscheid, T. Welton, Ionic Liquids in Synthesis, VCH-Wiley, Weinheim, 2002.

[3] H. Zhao, S.V. Malhotra, Aldrich Acta 35 (2002) 75.

[4] K.R. Seddon, J. Chem. Technol. Biotechnol. 68 (1997) 351.

[5] C. Baudequin, J. Baudoux, J. Levillain, D. Cahard, A.C. Gaumont, J.C. Plaquevent, Tetrahedron Asymmetr. 14 (2003) 3081–3093.

[6] L. Leclercq, I. Suisse, F. Agbossou-Niedercorn, Chem. Commun. (2008) 311–313.

[7] C.P. Mehnert, Chem. Eur. J. 11 (2005) 50–56.

[8] H.-U. Blaser, M. Studer, Green Chem. 5 (2003) 112–117.

[9] C.E. Song, Chem. Commun. (2004) 1033–1043.

[10] S. Park, R.J. Kazlauskas, Curr. Opin. Biotechnol. 14 (2003) 432–437.

[11] U. Kragl, M. Eckstein, N. Kaftzik, Curr. Opin. Biotechnol. 13 (2002) 565–571.

[12] C.F. Poole, J. Chromatogr. A 1037 (2004) 49–82.

[13] A.M. Stalcup, B. Cabovska, J. Liquid Chromatogr. Relat. Technol. 27 (2004) 1443–1459.

[14] M. Antonietti, D.B. Kuang, B. Smarsly, Z. Yong, Angew. Chem. Int. Ed. Engl. 43 (2004) 4988–4992.

[15] J. Dupont, J. Braz. Chem. Soc. 15 (2004) 341–350.

[16] C. M Gordon, J.D. Holbrey, A.R. Kennedy, K.R. Seddon, J. Mater. Chem. 8 (1998) 2627–2636.

[17] J. Dupont, P.A.Z. Suarez, R.F. de Souza, R.A. Burrow, J.P. Kintzinger, Chem. Eur. J. 6 (2000) 2377–2381.

[18] S. Saha, S. Hayashi, A. Kobayashi, H.-O. Hamaguchi, Chem. Lett. 32 (2003) 740–741.

[19] D.G. Golovanov, K.A. Lyssenko, M.Y. Antipin, Y.S. Vygoskii, E.I. Lozinskaya, A.S. Shaplov, Cryst. Eng. Comm. 6 (2005) 53–56.

[20] A. Getsis, A.-V. Mudring, Acta Crystallogr. E61 (2005) 2945–2946.

[21] J. Dupont, P.A.Z. Suarez, Phys. Chem. Phys. Chem. 8 (2006) 2441–2452.

[22] R.W. Alder, P.R. Allen, S.J.J. Williams, Chem. Soc. Chem. Commun. (1995) 1267–1268.

[23] T.L. Amyes, S.T. Diver, J.P. Richard, F.M. Rivas, K. Toth, J. Am. Chem. Soc. 126 (2004) 4366–4374.

[24] G.A. Jeffrey, An Introduction to Hydrogen Bonding, Oxford University Press, Oxford, 1997.

[25] L. Leclercq, A. R. Schmitzer, J. Phys. Chem. A, in press.

[26] G.R. Desiraju (Ed.), Crystal Design: Structure and Function. Perspectives in Supramolecular Chemistry, vol. 7, Wiley, Chichester, England, 2004, p. 6.

[27] P.B. Hitchcock, K.R. Seddon, T. Welton, J. Chem. Soc. Dalton Trans. (1993) 2639–2643.